ELSEVIER

Contents lists available at ScienceDirect

### Electric Power Systems Research

journal homepage: www.elsevier.com/locate/epsr





# Ground-based observations of lightning-related X-ray/gamma-ray emissions in Florida: Occurrence context and new insights

Vladimir A. Rakov \*, Istvan Kereszy

Department of Electrical and Computer Engineering, University of Florida, Gainesville, Florida, United States of America

#### ARTICLE INFO

Keywords:
Lightning
X-rays
Gamma-rays
Subsequent leader
Attachment process
Terrestrial gamma-ray flashes (TGFs)
Runaway electrons

#### ABSTRACT

Ground-based observations of energetic radiation (X-rays/gamma-rays) associated with natural lightning discharges are presented and discussed. The emphasis is placed on relating X-ray/gamma-ray emissions to specific lightning processes. X-rays/gamma-rays have been observed in the following three contexts: (1) final stages of the descending leader, (2) collision of opposite-polarity streamers at the onset of lightning attachments process, and (3) in-cloud processes giving rise to energetic radiation bursts characteristic of Terrestrial Gamma-ray Flashes (TGFs). In all three cases, the X-ray/gamma-ray production involves runaway electrons and can be materially influenced (enhanced) by the presence of previously created but decayed lightning channels. Such channels are characterized by elevated temperature (about 3,000 K vs. 300 K for ambient air), which significantly lowers the friction curve (representing the spatial rate of electron energy loss), so that its peak is an order of magnitude lower than that for cold air. As a result, in the electric field of about 4 MV/m (such and even higher fields are briefly produced near the tips of lightning leaders), ambient electrons can be accelerated over the friction-curve peak to the keV range and further to relativistic energies needed for production of X-ray/gammaray emissions. Significant avalanching of runaway electrons seems to be possible. For one very intense (55 kA) subsequent stroke, which was a prolific X-ray/gamma-ray producer, we estimated the spatial extent of strong (>4 MV/m) electric field region associated with the descending leader tip to be about 1.5 m, which is sufficient for multiplication of runaway electrons by a factor of  $2 \times 10^4$  or so.

#### 1. Introduction

At present, the only viable mechanism for producing energetic radiation by thunderstorms and lightning involves runaway electrons, which occur when the energy gained by free electrons between collisions, as they are accelerated by high electric field, exceeds the energy that is lost to collisions with air molecules. An X-ray/gamma-ray (in lightning research, the boundary between the two is usually placed at 1 MeV) photon is emitted when a free electron, passing by a nitrogen or oxygen atom, is deflected by the electric field of its nucleus or, to a lesser extent, by the field of its electrons. This process is called bremsstrahlung (braking radiation).

All observations of X-rays/gamma-rays associated with thunderstorms and lightning fall into three categories:

(a) surges in the gamma-ray background (gamma-ray glows) lasting seconds to minutes,

- (b) bursts of X-rays/gamma-rays associated with all kinds of descending leaders in natural and rocket-and-wire triggered lightning flashes, as they approach the ground, and
- (c) Terrestrial Gamma-ray Flashes or TGFs (typically less than 1 ms in duration), which originate from the cloud.

Gamma-ray glows have been reported from both ground-based (e.g., [8, 51, 54]) and airborne observations (e.g., [22, 29, 32, 37]). The energy spectrum is thought to extend to some tens of MeV. The source of gamma-ray glows is a high-electric-field region in the cloud (for example, between the main negative and lower positive charge layers), where energetic (0.1–1 MeV) electrons produced in the atmosphere by very high energy cosmic rays are accelerated forming runaway electron avalanches. When observed at ground level, usually when the distance between the in-cloud charged-particle accelerator and ground-based detector is small (high-elevation observation site or low-altitude winter thunderclouds), they are also referred to as Thunderstorm Ground Enhancements (TGEs). Note that TGEs were identified with

E-mail address: rakov@ece.ufl.edu (V.A. Rakov).

<sup>\*</sup> Corresponding author.

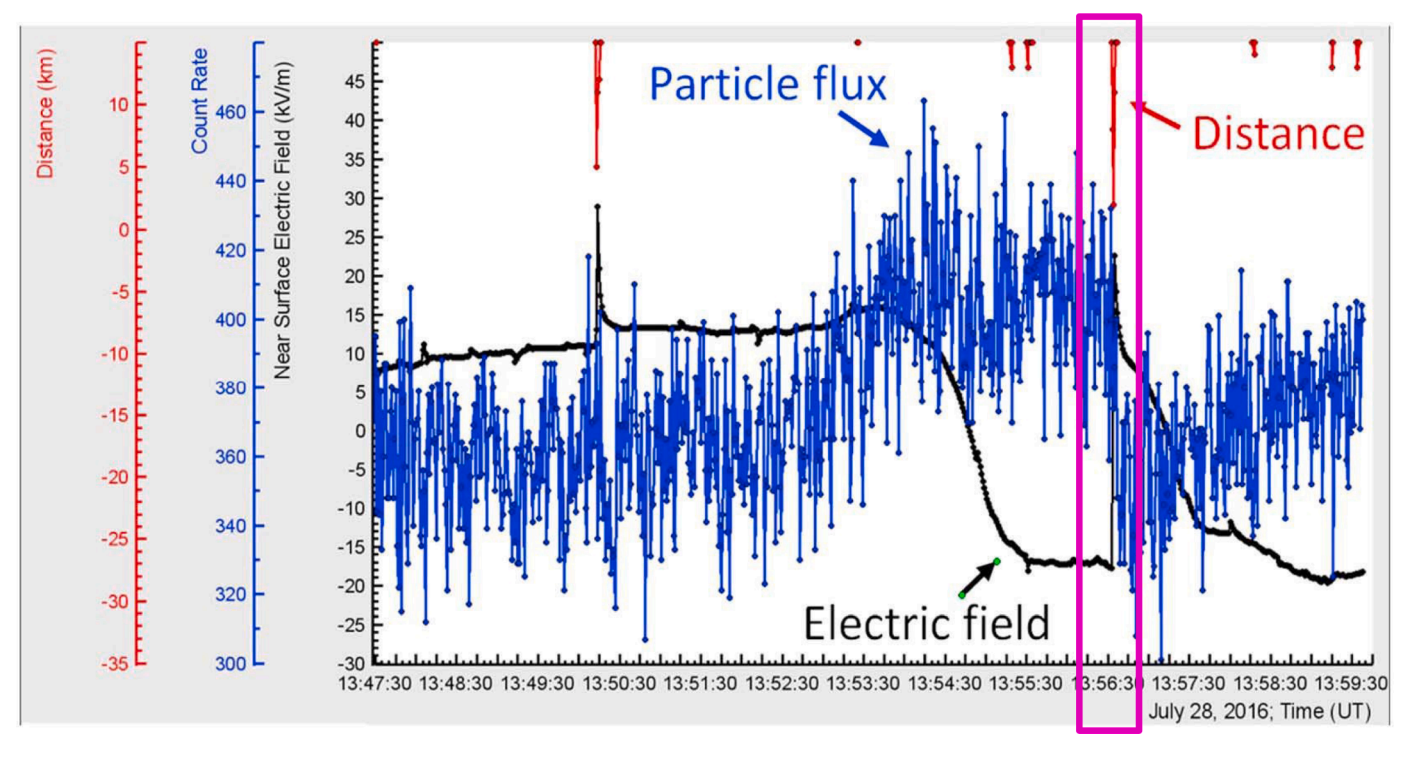


Fig. 1. Gamma-ray glow/TGE, shown in blue and labeled "Particle flux" ("Count Rate", per second, on the blue vertical axis), recorded on Mount Aragats (3.2 km above sea level), Armenia, that was terminated around 13:56:30 UT (inside the vertically elongated magenta box) by a negative cloud-to-ground lightning flash (-CG). The TGE was about 20% above the background and its duration was about 4 min. The corresponding electric field variation is shown in black; its abrupt upward excursion and polarity reversal signify the removal of dominant negative charge (accelerating electrons in the downward direction) aloft. Distance to the -CG (shown in red) was about 2 km. Adapted from Chilingarian et al. [10]. (For interpretation of the references to colour in this figure legend, the reader is referred to the web version of this article.)

particle detectors [8] and besides gamma rays generally include energetic electrons and neutrons. Gamma-ray glows/TGEs are often terminated by lightning that suddenly removes their causative electric field (e.g., [10, 11]), as illustrated in Fig. 1.

It is thought that TGEs can be produced by two processes, RREA (relativistic runaway electron avalanches) and MOS (modification of energy spectrum of cosmic-ray secondaries) ([9, 5]). RREA can occur in regions where the electric field exceeds a threshold of 284 kV/m (at sea level) over a distance comparable to the avalanche length (tens to hundreds of meters) with a minimum potential difference of 7.3 MV (e. g., [21]). Only MOS occurs below the RREA field threshold and both RREA and MOS can occur above that threshold.

It is worth noting that a long-lasting enhancement of energetic radiation relative to the background level can also occur as a result of the so-called radon washout effect (e.g., [7, 41]); that is, in the absence of an in-cloud electron accelerator. It is associated with precipitation that scavenges airborne radionuclides (mostly short-lived radon-222 progeny) to the ground. Energies of radon-related emissions are thought to be below 3 MeV (e.g., [50]).

Gamma-ray glows and other long-lasting energetic radiation enhancements (briefly reviewed here just for completeness) are no further discussed in this paper.

Lightning leaders observed at close ranges (within 2 km or so) often produce detectable X-ray/gamma-ray emissions. A number of studies have shown that both natural (e.g., [19, 36, 38, 52]) and rocket-and-wire triggered (e.g., [16, 20, 47]) lightning can produce such emissions. They were observed during stepped, dart-stepped, and dart leaders (also during less common chaotic leaders), usually within 1 ms prior to the return-stroke onset, when the leader tip is within a few hundred meters of the ground. While the typical photon energy is in the tens to hundreds of keV ranges, individual photons with energies exceeding several MeV have been documented.

TGFs are mostly observed from space (e.g., [6, 23, 40, 49]) and relatively infrequently seen at the ground. TGFs recorded at ground level are referred to as downward TGFs. To date, downward TGFs were observed in Florida, Utah, and Japan. For TGFs observed from space, the energy spectrum is thought to extend to some tens of MeV, while for downward TGFs it seems to be somewhat softer.

In the following, we will present recent ground-based observations of X-rays/gamma-rays either produced by natural-lightning processes near ground (final stage of descending leader or ground attachment) or by some in-cloud processes giving rise to an energetic radiation burst indicative of TGF, this burst being concurrent with a natural cloud-to-ground lightning discharge. The emphasis will be placed on relating X-ray/gamma-ray emissions to specific lightning processes. We will also identify the lightning channel properties and leader parameters that are conducive to the production of energetic radiation. The results are important for improving our understanding of the physics of lightning, in particular its processes occurring in the presence of preconditioned channels/branches. All the data were acquired at the Lightning Observatory in Gainesville (LOG), Florida. The paper is based on (is an extended version of) the invited lecture [43] given by the authors at the ICLP-SIPDA 2021 in Colombo, Sri Lanka.

#### 2. Instrumentation

As noted above, all the data presented in this paper (except for Fig. 1) were obtained at the Lightning Observatory in Gainesville (LOG), Florida. Those data, besides the X-ray/gamma-ray records, also include electric field (E), electric field derivative (dE/dt), and magnetic field derivative (dB/dt) waveforms. LOG is located on the roof of the five-story New Engineering Building (NEB) on the University of Florida campus (see Fig. 2).

The E-field measuring system included a 0.155 m<sup>2</sup> flush-mounted

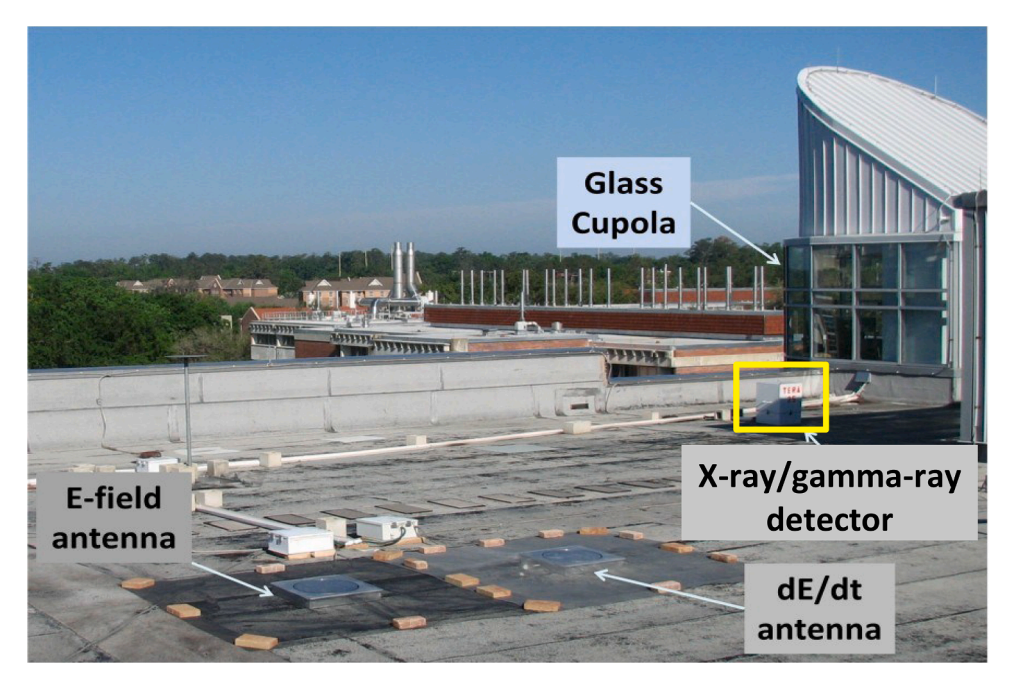


Fig. 2. South Side of the Lightning Observatory in Gainesville (LOG), Florida.

 Table 1

 Acceleration and multiplication of runaway electrons in air.

	_	-	
Process	Source of seed electrons	Air temperature, K	Electric field,* $MV/m$
Relativistic avalanches in c air (cold runav breakdown)		300	≳ 30
Relativistic avalanches in o air (RREA)	Cosmic-ray cold secondaries	300	~ 0.2
Relativistic avalanches in remnants of decayed chann	Ambient distribution nel	3000	≥ 3
Conventional (no relativistic) avalanches in o air	distribution	300	~3

<sup>\*</sup>Approximate values at sea level.

flat-plate antenna followed by a unity gain, high-input-impedance amplifier with an active integrator. The E-field enhancement factor due to the presence of NEB was estimated to be 1.4 [1]. The E-field measuring system (one of the two, with a lower gain) had a useful frequency bandwidth of 16 Hz to 10 MHz, with a decay time constant of 10 ms. The output signal was transmitted through a fiber-optic link to a digitizing oscilloscope which sampled at 100 MHz. The dB/dt antenna was a vertical loop with an area of 0.533 m². Its plane was oriented in the east-west direction. The dB/dt measuring system had a -3 dB upper frequency response of 16 MHz. The E and dB/dt records were used to identify different lightning processes, determine the return-stroke onset times, and estimate leader durations.

The X-ray/gamma-ray detector consists of a NaI(Tl) scintillator of cylindrical shape with both its height and diameter equal to 7.6 cm coupled to a photomultiplier tube (PMT) and associated electronics. The detector was powered by a 12 V battery and housed in an aluminum box with a wall thickness of 0.32 cm that shielded it from electromagnetic coupling, moisture, and light, but allowed photons with energies down to 30 keV to enter. The detector's output signal was transmitted through

a fiber-optic link to the digitizing oscilloscope which sampled at 100 MHz. The 662 keV photons emitted by a radioactive source (Cs-137) were used to calibrate the detector. The upper and lower measurement limits of the detector (determined by the voltage range of the fiber-optic link and the noise level) were 5.7 MeV and 75 keV, respectively. Using this detector, Mallick et al. [36] estimated the occurrence of detectable background (not lightning related) X-rays/gamma-rays at LOG to be 1 in 8 ms.

#### 3. Data presentation and results

We first discuss, in subSection 3.1, X-rays/gamma-rays associated with descending leaders and with the lightning attachment process and then Terrestrial Gamma-ray Flashes (TGFs) in subSection 3.2.

## 3.1. X-rays/gamma-rays associated with descending leaders and with the attachment process

Mallick et al. [36] discovered that subsequent-stroke leaders in natural negative lightning discharges could be more prolific producers of X-rays/gamma-rays than the first-stroke leader in the same flash, even when the peak current reported by the NLDN (U.S. National Lightning Detection Network) for the subsequent stroke was comparable to or lower than that for the first stroke. In their study, conducted at LOG, five out of seven subsequent-stroke leaders produced more detectable X-ray/gamma-ray pulses than their corresponding first-stroke leaders. An example of such an event is shown in Fig. 3. They used the relatively short subsequent-leader durations measured in their electric field and electric field derivative records to argue that their subsequent leaders followed the same path to ground as the first leader, as opposed to deviating from the previously formed channel and forging a new path to ground through cold air. Later, Tran et al. [52], also working at LOG, presented optical evidence that subsequent strokes following previously formed channels can indeed produce more X-rays/gamma-rays than the corresponding first stroke.

Mallick et al. [36] and Tran et al. [52] attributed their findings to the fact that normal subsequent-stroke leaders traverse channels whose air density is considerably lower than that of the virgin air in which first-stroke leaders have to develop. Their implicit assumption was that the only difference between the first- and subsequent-leader paths in

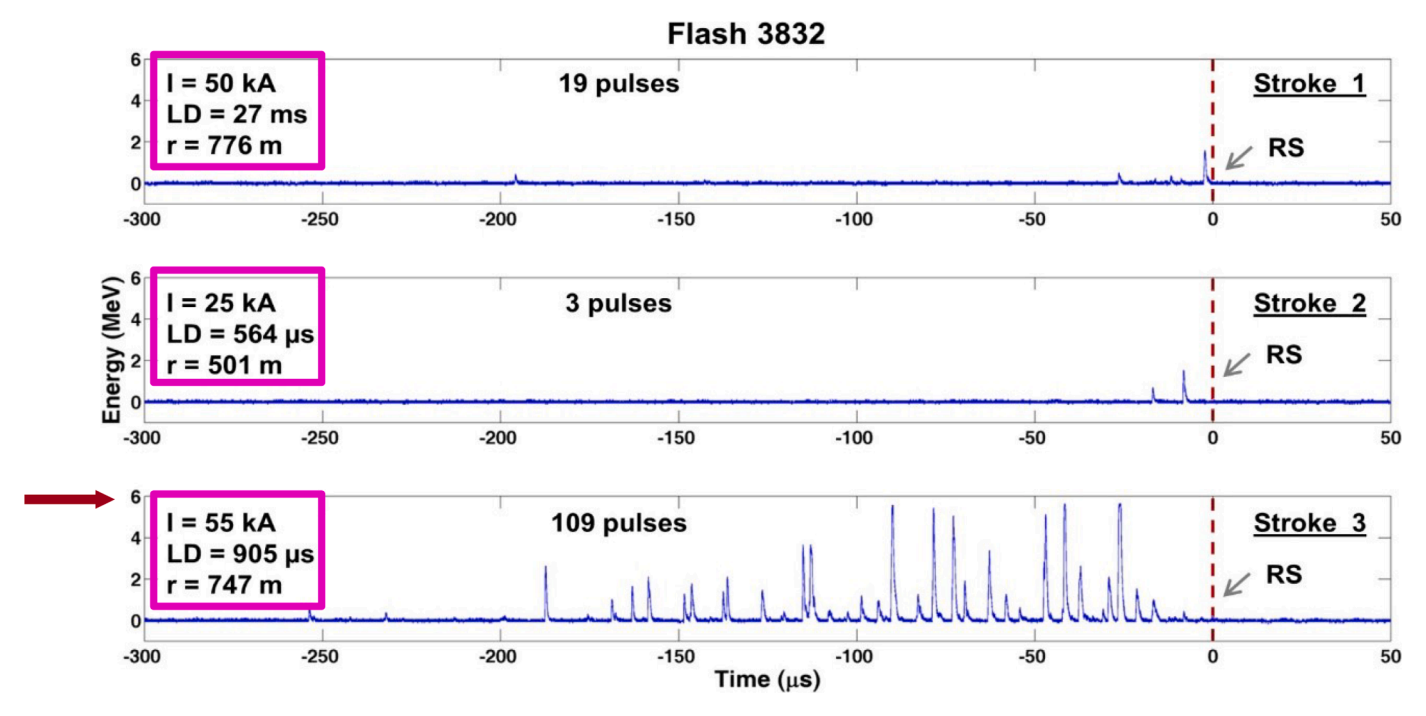


Fig. 3. X-rays/gamma-rays produced by Stroke 1 (top), Stroke 2 (middle), and Stroke 3 (bottom) of 13-stroke Flash 3832. Strokes 4 to 13 were not recorded at LOG. NLDN-reported distances for strokes 1 to 3 were 0.5 to 0.8 km. Vertical broken lines labeled RS indicate the position of the return stroke. Some pulses seen in the plots are due to multiple photons arriving within the response time of the X-ray/gamma-ray detector; that is, are actually each a superposition (pile-up) of two or more individual pulses. There are a total of 22 such pile-ups, 3 of which are clipped at 5 to 6 MeV level. All discernible individual pulses are included in the pulse count given on the plots. Adapted from Mallick et al. [36].

their studies was the air temperature (ambient, 300 K, for first leaders vs. about 3000 K for subsequent leaders), with the total particle density at 1-atm pressure for the latter being about an order of magnitude lower than for the former [55]. This an order of magnitude difference in air density results in the lowering by an order of magnitude the friction force (rate of electron energy loss per unit distance) relative to the ambient (cold) air case, as further discussed in Section 4.

X-ray/gamma-ray emissions have been also observed during the lightning attachment process, at the time of collision of negative and positive streamers of the descending and upward connecting leaders, respectively [28, 52]. One example is shown in Fig. 4, where energetic radiation is seen in coincidence with the so-called leader burst (LB), but not with the leader step pulses (marked in panels (a) and (b)). The LB occurs at the beginning of the breakthrough phase (part of the attachment process), when the leaders collide via their streamer zones and form the common streamer zone. This corresponds to the beginning of the slow front in electric field waveforms (marked in Fig. 4a). More details on the breakthrough phase and its relation to the return-stroke slow front can be found in work of Rakov and Tran [44].

To summarize, it appears that X-rays/gamma-rays can be produced in the course of leader stepping and in the course of collision of opposite polarity leaders during the lightning attachment process. On the other hand, not every leader step is associated with a detectable X-ray/ gamma-ray burst (see, for example, Fig. 4, where none of the four marked step pulses produced an energetic radiation burst) and there can be detectable emission in the absence of detectable stepping as, for example, in the case of dart leaders. Clearly, further research is needed to distinguish the absence of energetic radiation at the source from an insufficient X-ray/gamma-ray flux toward the detector, as well as to better understand the nature of energetic radiation from dart (nonstepped) leaders. It has been suggested (e.g., [27]) that X-rays/gamma-rays from stepped or dart-stepped leaders are associated with the corona streamer burst (see, for example, Fig. 2 of Kostinskiy et al. [33]) completing the formation of each step. Dart leaders apparently do not produce such bursts, but should have a kind of guided streamer zone ahead of the leader tip. Moss et al. [39] suggested that super-fields briefly occurring near streamer heads can serve to accelerate some ambient electrons to energies in the 2–8 keV range and that the latter can be further accelerated to relativistic energies (up to tens of MeV) in a larger-scale field of the corona streamer burst. Note that Moss et al.'s scenario applies to stepped leaders in cold air. It has been shown (e.g., [12, 13, 31]) that the Coulomb force associated with a descending subsequent leader can overcome the friction force in warm air without considering any streamer processes near the leader tip.

#### 3.2. Terrestrial gamma-ray flashes (TGFs)

Tran et al. [53] reported on a TGF observed in 2014 at the Lightning Observatory in Gainesville (LOG), Florida. It was associated with a single-stroke 224 kA -CG at a distance of 7.5 km from LOG. The TGF had a duration of 16 µs and was composed of 6 detectable photons, four of which were in the MeV-range, with two exceeding the 5.7 MeV saturation level (reaching 13 MeV after pulse reconstruction). It is shown, along with the corresponding wideband electric field and electric field derivative (dE/dt) records, in Fig. 5. The E-field and dE/dt records are shown using the atmospheric electricity sign convention (e.g., [45], Section 1.4.2), according to which the downward directed electric field or electric field change vector is assumed to be positive. Besides the RF electromagnetic field signatures recorded at LOG, electric field waveforms at larger distances (not shown here) recorded by the U.S. National Lightning Detection Network (NLDN) and the Earth Networks Total Lightning Network (ENTLN) were also examined. The TGF occurred 202 μs after the return-stroke onset and was accompanied by a dE/dt burst (marked in Fig. 5b). The temporal coincidence of TGF and dE/dt burst was reported by Tran et al. [53] for the first time and suggested that relativistic processes responsible for the TGF production and the low-energy streamer formation process responsible for the dE/dt burst can be taking place concurrently.

Essentially no energetic radiation was seen prior to the return-stroke onset (during the preliminary breakdown and stepped leader stages).

X-ray pulse associated with the attachment process (the beginning of the breakthrough phase).

Note the absence of detectable x-rays associated with leader steps.

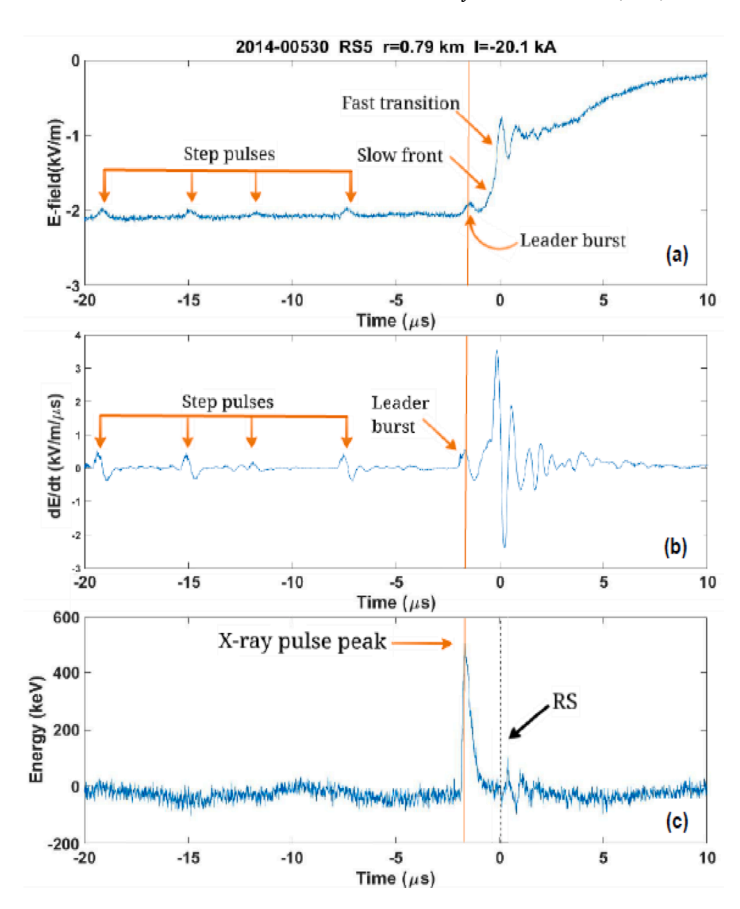


**Fig. 4.** Flash 2014–00530. (a) Electric field, (b) dE/dt, and (c) X-ray records for Stroke 5. Only one detectable X-ray pulse was produced by this stroke, which occurred in coincidence with the leader burst (LB) seen at the beginning of the slow front marked in (a). The occurrence of the X-ray pulse at the time of LB suggests that the X-ray emission was associated with the collision of streamer zones of opposite polarity of the downward negative leader and upward positive connecting leader. Solid vertical lines in (a), (b), and (c) indicate the position of the LB peak in (b). Broken vertical line at t = 0 in (c) indicates the position of initial electric field peak in (a). Adapted from Tran et al. [52]. (For interpretation of the references to colour in this figure legend, the reader is referred to the web version of this article.)

The stepped-leader duration was as short as 3.9 ms, which, according to Zhu et al. [58], indicates that the leader was about an order of magnitude faster than typical stepped leaders in -CGs. The lack of detectable X-rays/gamma-rays from leader steps is likely related to the relatively large distance (7.5 km) from the channel to ground, even though the RS peak current (and by inference leader tip potential) was very high. The process giving rise to the observed TGF probably occurred inside the cloud and involved a branch at a considerably smaller distance from the detector than the channel to ground. For comparison, the TGF producer reported by Dwyer et al. [18] was an intense (99 kA) first (and the only) stroke in a -CG, whose stepped-leader emitted a copious amount of X-rays/gamma rays at a distance of 800 m. The TGF had a duration of 53  $\mu$ s, was composed of 19 pulses, and started 191  $\mu$ s after the RS onset, very similar to the TGF reported by Tran et al. [53] and discussed above.

We now present the most recent Florida TGF, which was recorded at LOG in 2018 and occurred in a rather unusual context, between opposite polarity strokes of a bipolar cloud-to-ground lightning flash. Bipolar lightning discharges sequentially transfer to ground both positive and negative charges during the same flash [42]. They constitute about 10% of the global lightning activity. The flash in question created a total of three channels to ground, the first one taken by Stroke 1 only, the second one taken by Strokes 2 and 3, and the third one by Strokes 4 and 5. The overall E-field, dB/dt, and X-ray/gamma-ray records of this flash are shown in Fig. 6. The E-field record is shown using the atmospheric electricity sign convention (e.g., [45], Section 1.4.2), according to which the downward directed electric field or electric field change vector is assumed to be positive.

Data for Stroke 3 (TGF producer) are shown on expanded time scales

in Figs. 7 and 8. Based on the NLDN data, 28 kA Stroke 3 followed the remnants of the channel to ground created by  $12\,\mathrm{kA}$  Stroke 2, about 200 m from LOG. This is confirmed by the <3-ms duration of the leader of Stroke 3 (see Fig. 7a and b), which is characteristic of a leader developing in previously created channel (leaders creating a new channel to ground usually have durations of the order of tens of milliseconds). Kereszy et al. [30] inferred from the entirety of their data that the negative leader initiating Stroke 3, while developing inside the cloud along the residual channel of Stroke 1, entered the remnants of the warmer channel to ground created by Stroke 2 (the time elapsed since the RS of Stroke 2 was 10 ms, considerably shorter than 22 ms elapsed since the RS of Stroke 1), where that negative leader produced the TGF marked in Figs. 6c, 7c, and 8b.

The TGF had a duration of 35  $\mu s$  and consisted of 18 pulses with amplitudes ranging from 114 to 912 keV. The energy spectrum of this TGF is considerably softer than for the one presented in Fig. 5a, where the average energy is about 5 MeV vs. some hundreds of keV for the event presented in Fig. 8b. This disparity implies that there is no characteristic energy spectrum for downward TGFs. Mailyan et al. [35] studied energy spectra of individual TGFs observed from space (upward TGFs) and found them to exhibit considerable diversity.

The leader of Stroke 3 also produced X-ray pulses characteristic of the stepping process (marked in Fig. 7c), which implies that it was a dart-stepped leader (although dart leaders are also known to produce X-rays as they approach the ground). The pattern of the X-ray-pulse sequence associated with leader stepping near ground was very different from that of the TGF. Specifically, the 15 leader-step pulses that occurred over about 700  $\mu$ s were separated by time intervals ranging

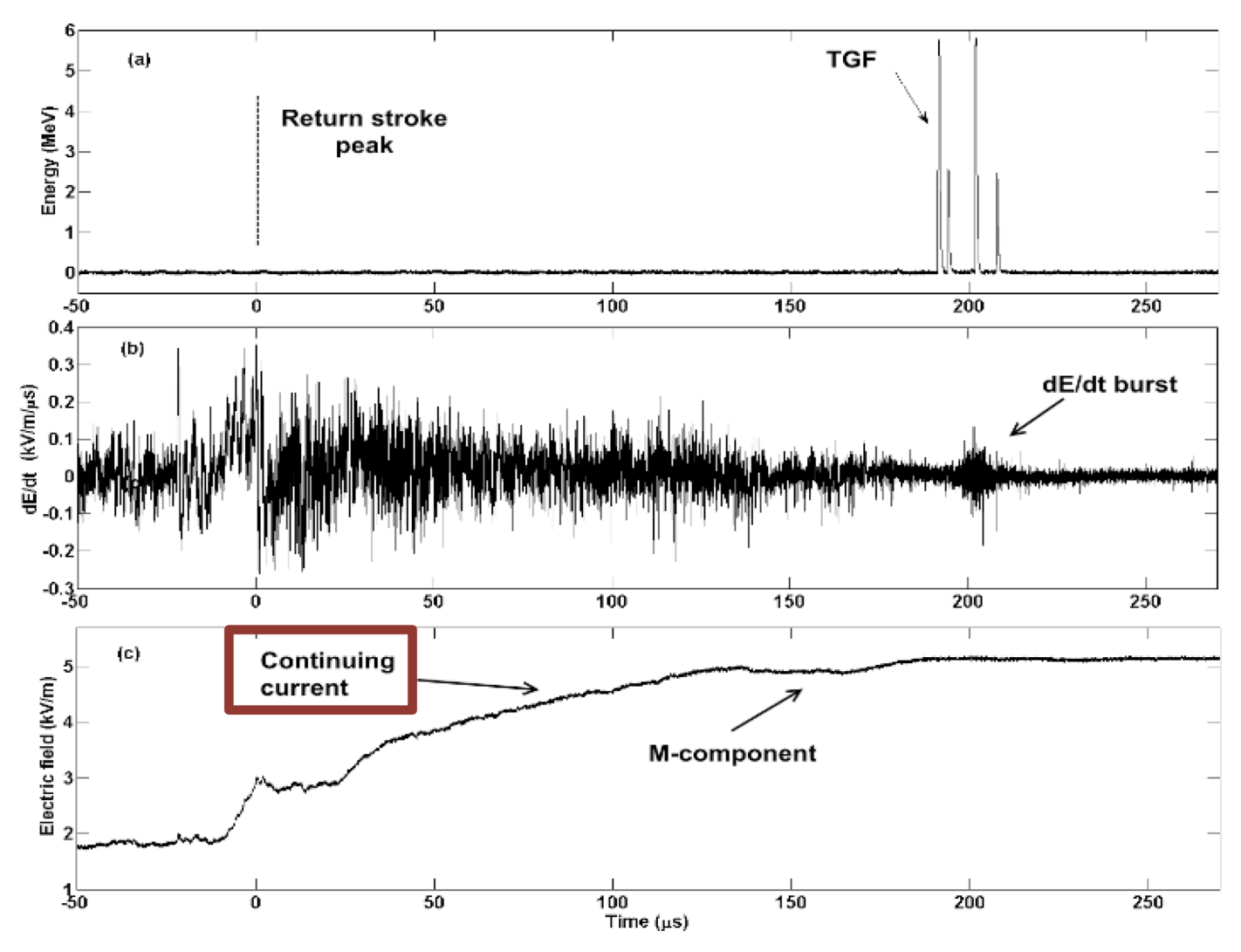


Fig. 5. (a) TGF observed at LOG on June 13, 2014, (b) dE/dt and (c) electric field signatures, also recorded at LOG (7.5 km from the lightning channel). t = 0 corresponds to the return-stroke (RS) initial field peak (marked in (a)), with the RS field risetime being 11 μs. Full time scale is 320 μs. The TGF occurred 202 μs after the RS onset, during the 20 ms continuing current. Adapted from Tran et al. [53]. (For interpretation of the references to colour in this figure legend, the reader is referred to the web version of this article.)

from 6.6 to 177  $\mu s$  (mean  $=47~\mu s$ ) and tended to increase in amplitude as the leader was approaching the ground (moving into the increasing electric field region). In contrast, the TGF was a compact (35  $\mu s$ ) burst with interpulse intervals ranging from 0.9 to 7.7  $\mu s$  (mean  $=1.9~\mu s$ ) and pulse amplitudes showing an increasing trend followed by an irregular variation (see Fig. 8c). This disparity suggests that the TGF was not associated with leader stepping, but rather with the negative in-cloud leader entering the upper part of a warmer channel to ground created by the preceding stroke and encountering a relatively sharp air-density gradient (probably related to the relative age of the residual channels of Strokes 1 and 2) there.

Besides the two Florida TGFs described above, ground-based TGF observations in Florida include three events recorded at Camp Blanding, two associated with rocket-and-wire triggered lightning [17, 25] and one with natural lightning [18]. All those three events, as well the one recorded at LOG in 2014 (see Fig. 5), occurred in the presence of steady current carrying negative charge to ground, well after the flash initiation processes. The Florida TGF that was recorded at LOG in 2018 also occurred long after the onset of the flash (see Fig. 6).

In contrast, Belz et al. [4] reported TGFs associated with the initial (preliminary) breakdown or first-leader process from recent ground-based observations in Utah. NLDN-reported peak currents, inferred from the RF field signatures of the initial breakdown, were a few

tens of kiloamperes. TGFs occurring in a similar context, but in association with larger-amplitude (>100 kA) intracloud (IC) pulses were also observed at ground level during winter thunderstorms in Japan. Specifically, the context of two TGFs presented by Wada et al. [[56], [57]] and one TGF presented by Hisadomi et al. [26] was described by the authors as a gamma-ray glow (typical duration of the order of minutes; see Section 1 of this paper) terminated by a lightning discharge producing a wideband RF electromagnetic field signature referred to as "negative energetic intracloud pulse" or -EIP associated with negative charge moving downward (the term EIP was introduced by Lyu et al. [34]). The magnitudes of the associated peak currents were estimated to be 260 and 197 kA in Wada et al. [57] and 122 kA in Hisadomi et al. [26]. The nature of EIPs is presently not clear.

#### 4. Discussion

As noted in the Introduction, the X-ray/gamma-ray emission occurs when runaway electrons experience deflection by the electric field of other charged particles (typically atomic nuclei), the process that is referred to as Bremsstrahlung or braking radiation. The rate of electron energy loss per unit distance is often called the friction force and its dependence on electron energy is represented by the so-called friction curve. Two such curves, for cold air and for air at 3000 K, are shown in

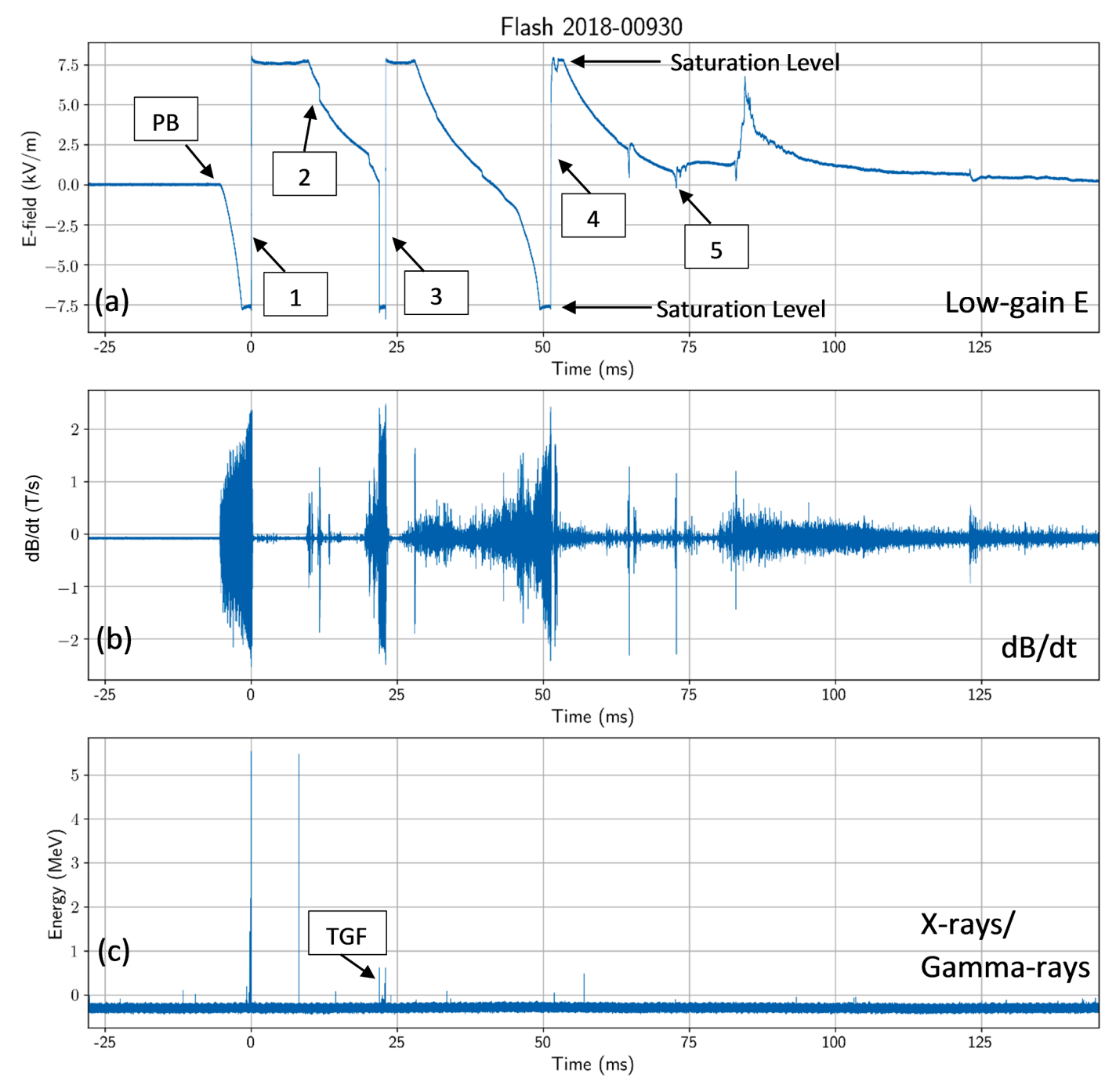
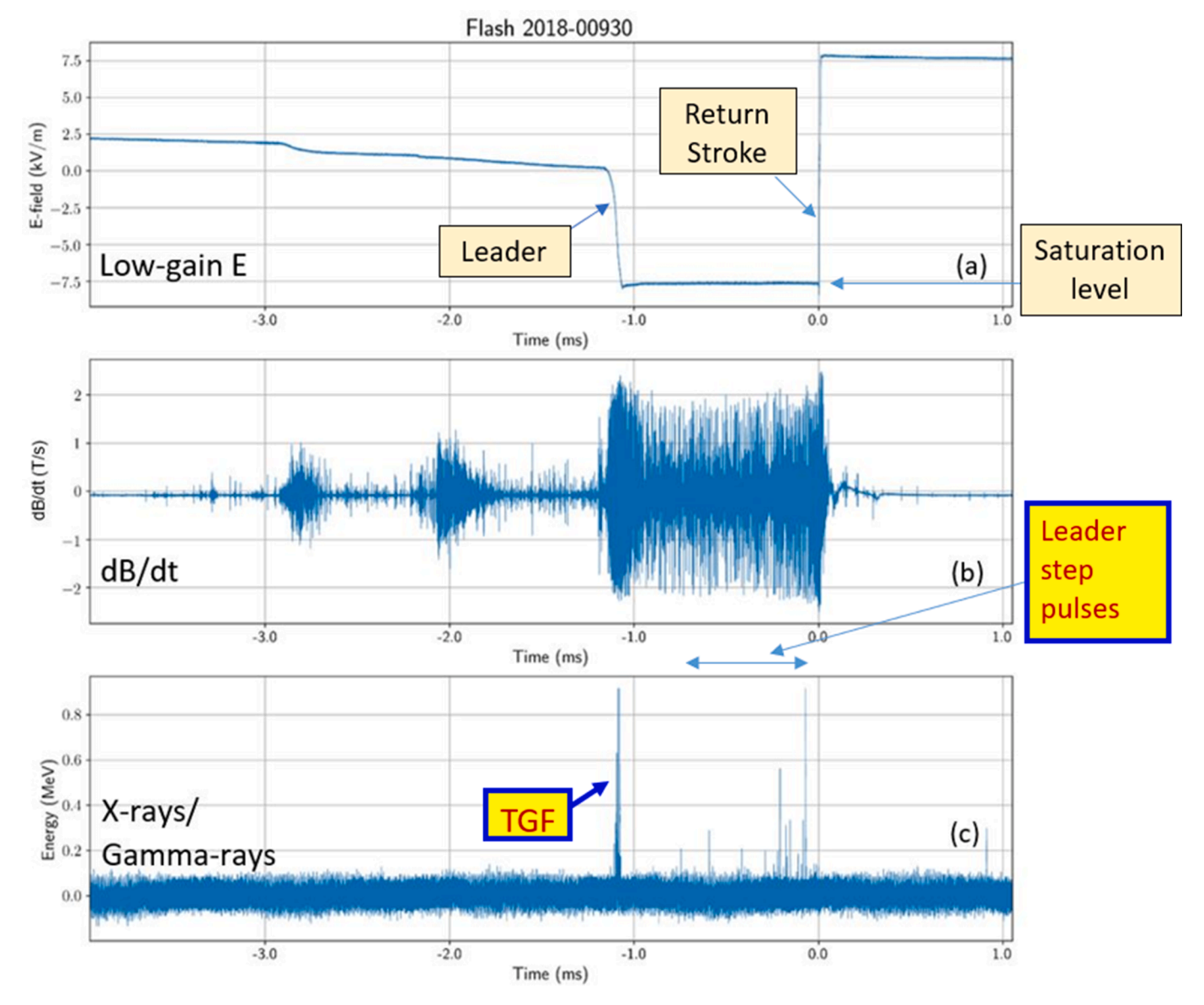


Fig. 6. Overall records of (a) low-gain electric field ( $\tau=10$  ms), (b) magnetic field derivative (dB/dt), and (c) X-rays/gamma-rays for the five-stroke bipolar flash during which the TGF recorded at LOG in 2018 occurred. In (a), PB stands for the preliminary breakdown and the boxed numbers indicate stroke order. Leaders of Strokes 1 and 3 produced X-ray/gamma-ray bursts as they approached ground, but no energetic radiation was detected during PB. Full time scale is 175 ms. t=0 corresponds to the onset of the return-stroke stage of Stroke 1. Adapted from Kereszy et al. [30]. (For interpretation of the references to colour in this figure legend, the reader is referred to the web version of this article.)

Fig. 9.

Table 1 compares the various scenarios of acceleration and multiplication of runaway electrons in terms of the source of seed electrons, air temperature, and characteristic electric field. Conventional (non-relativistic) avalanches are additionally included in the last row, as a reference. In Table 1, the ambient electron-energy distribution includes electrons with energies less than 30 eV or so, while the so-called cosmic-ray secondaries (electrons produced by very high energy  $(10^{15}-10^{16} \ eV)$  or greater) cosmic-ray particles) have energies exceeding 0.1–1 MeV. For comparison, the average energy of electrons in conventional electric

breakdown is just a few electron-volts. It follows from Table 1 that there are three main factors/scenarios that can lead to acceleration and multiplication of runaway electrons: (1) super-high electric field (much higher than the conventional breakdown value), (2) energetic electrons supplied by external sources (cosmic rays), and (3) elevated air temperature (reduced air density). Scenario 1 is referred to as cold runaway breakdown and Scenario 2 as relativistic runaway electron avalanches (RREAs). Referring to Fig. 9, Scenario 1 relies on lifting the horizontal line representing the Coulomb force above the friction-curve peak and Scenario 3 on lowering the friction curve so that it is peak is below the



**Fig. 7.** Same as Fig. 6, but for Stroke 3 (TGF producer), shown on expanded (5 ms) time scale. Stroke 3 was negative and followed the channel created by Stroke 2 (positive) at a distance of 200 m from LOG. TGF, marked in (c), is shown on a 110 μs time scale in Fig. 8. t = 0 corresponds to the onset of the return-stroke stage of Stroke 3. Also marked in (c) are leader step pulses (X-rays/gamma-rays associated with the leader of stroke 3). Adapted from Kereszy et al. [30].

Coulomb-force line, without imposing any requirement on the energy of seed electrons. In contrast, Scenario 2 requires the presence of energetic electrons supplied by an external agent.

The cold runaway breakdown and RREA are widely discussed in the literature (e.g., [15, 24, 39]), while the elevated-temperature scenario is relatively new. It was first introduced by Mallick et al. [36] and further elaborated and discussed by Tran et al. [52,53] and Kereszy et al. [30, 31]. The elevated-temperature scenario requires the presence of pre-conditioned (decayed by still warm) channel. Such channels/branches are abundant in both cloud-to-ground (CG) and cloud (IC) discharges, and they are often traversed by transients carrying high electric potentials. For example, subsequent leaders in negative CGs typically develop along warm (reduced air density) channels for which the critical electric field needed to overcome the friction curve is about an order of magnitude lower than in cold air (compare the first and next to the last rows of Table 1). In the following, we present the calculated electric field waveform produced by a descending subsequent-stroke leader to demonstrate that the corresponding Coulomb force can be high enough to overcome the friction force for warm air, as per the 3000 K (red) friction curve shown in Fig. 9.

Kereszy et al. [31] found from modeling that the electric field near the descending leader tip strongly depends on the prospective return-stroke peak current (a proxy for the leader tip potential) and leader propagation speed. Specifically, the peak of electric field waveform increases with increasing the return-stroke current peak and with decreasing the leader speed. For a typical subsequent stroke, the electric field peak is a few MV/m, comparable to the electric field required for ambient electrons to run away in a warm (3000 K) channel (see next to the last row of Table 1). This means that even ordinary subsequent strokes are capable of producing energetic radiation in the absence of super-fields (≥ 30 MV/m) or energetic (0.1–1 MeV) electrons produced by external agents. For subsequent strokes with higher return-stroke peak currents and lower leader propagation speed (but still in the observed ranges of their variation), the electric field peak can briefly reach a few tens of MV/m, as shown in Fig. 10. Details of the leader model used are found in Kereszy et al. [31].

The event presented in Fig. 10 can be viewed as representing the very intense X-ray/gamma-ray producer presented in Fig. 3 (bottom panel) of

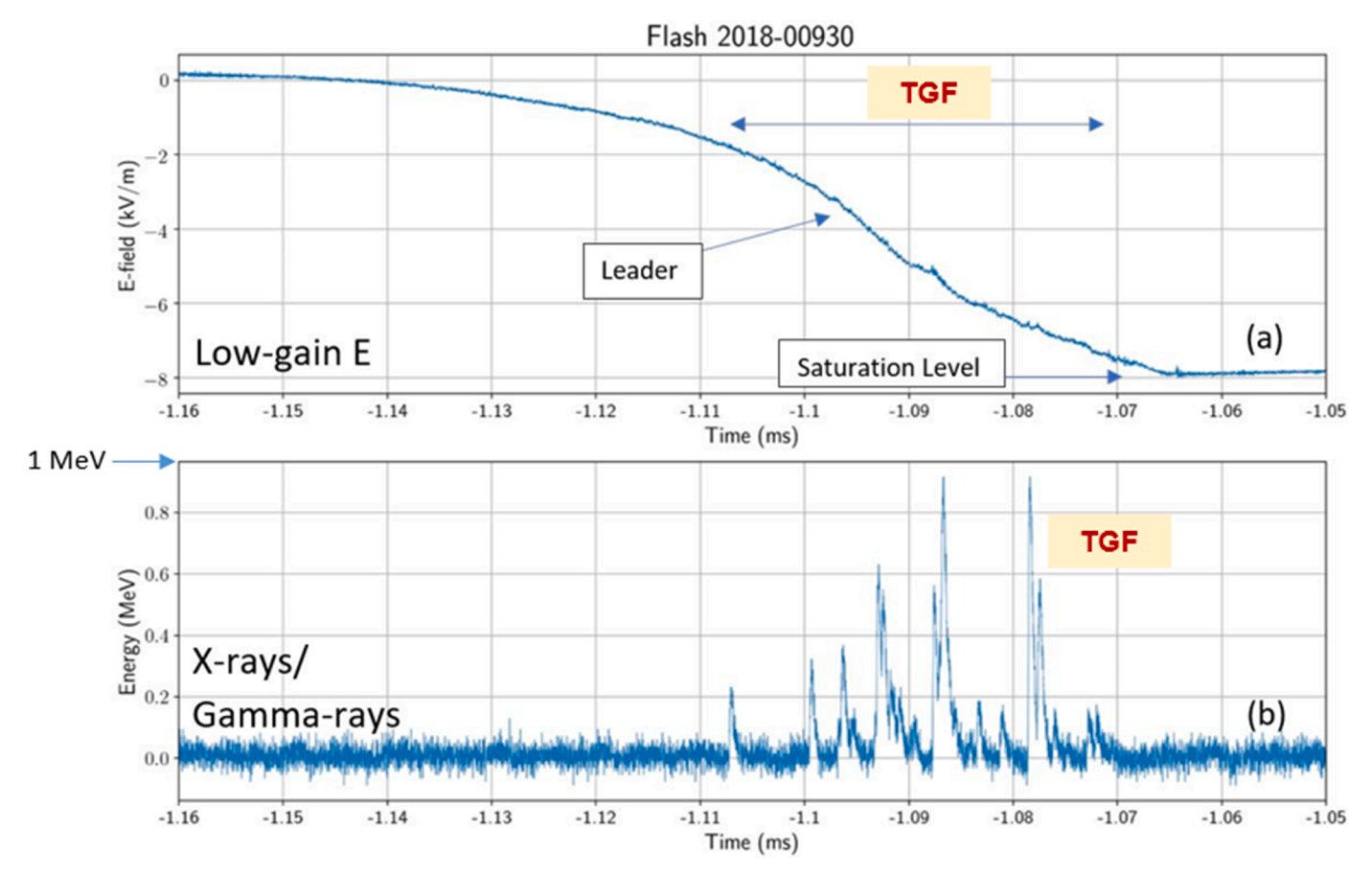


**Fig. 8.** (a) Electric field waveform corresponding to the initial stage of the leader of Stroke 3 (negative). (b) TGF inferred to be associated with an in-cloud part of Stroke 3 (negative leader entering the decayed but still warm channel to ground created by Stroke 2 (positive)). t = 0 corresponds to the onset of the return-stroke stage of Stroke 3. Full time scale is 110 μs. Adapted from Kereszy et al. [30].

this paper. That stroke followed the previously formed (warm) channel to ground and had the NLDN-reported peak current of 55 kA (same as in Fig. 10) and the leader speed  $\nu=8.3\times10^6$  m/s. This leader speed is inferred from the measured leader duration of 0.9 ms and assumed total channel length of 7.5 km. It is not too far from the value,  $\nu=5\times10^6$  m/s, used in computing the electric field waveform shown in Fig. 10. The stroke whose X-ray/gamma-ray emission is shown in the bottom panel of Fig. 3 produced at least one individual photon with energy exceeding 5 MeV (the highest recorded to date for subsequent-stroke leaders). The total number of detectable energetic-radiation pulses was 109, with about 80% of them showing no evidence of piling-up. If we neglect the piling-up effect, 13% of the 109 pulses exceed the 2 MeV level and 6% exceed the 4 MeV level.

As seen in Fig. 10, the calculated electric field peak at the descending leader tip for a subsequent stroke with  $I_p = 55$  kA and  $v = 5 \times 10^6$  m/s is 20 MV/m. The corresponding Coulomb force acting on an electron is considerably larger than the peak of the friction curve for warm air (corresponding to ~4 MV/m; see red curve in Fig. 9), which allows ambient free electrons to run away. Thus, as noted above, a runaway process does not require the presence of a super-energetic cosmic-ray particle and can start from the ambient electron distribution. Further, super-high electric fields (≥ 30 MV/m; see row 1 in Table 1) are not required in warm air either; a relatively low field of ~4 MV/m (even lower if the tunneling effects [14] are included) should be enough. Conventional electron avalanches in remnants of a decayed channel will occur at a field of about 300 kV/m, a factor of 10 lower than in cold air, providing abundant seeds for a thermal runaway process accelerating ambient electrons over the peak of the red friction curve in Fig. 9 to the keV energy range, which are further accelerated, via a relativistic runaway process, to the MeV range. The rise of electric field from 300 kV/m to 4 MV/m is very fast (much less than 1  $\mu s$ ; see Fig. 10), so that no significant field reduction due to conventional breakdown should occur. According to Bakhov et al. [[3], Fig. 7], the runaway delay time in strong (24–40 MV/m in nitrogen under normal conditions) electric fields, defined as the time necessary for the first electron with energy of a few keV to emerge from the ambient electron distribution, is very small, of the order of 0.01 ns.

The E-field vs. time waveform in Fig. 10 has a half-peak with of 90 ns, a width at the 4 MV level of 290 ns, and 710 ns at the 2 MV/m (10% of peak) level. Assuming that the magnitude and shape of the E-field pulse, as it travels along the channel, do not change much with height, we can obtain the corresponding spatial waveform parameters by multiplying the above time intervals by the leader extension speed of  $5 \times 10^6$  m/s. The resultant E-field vs. distance pulse is 3.6 m wide at the 2 MV/m level, and its part within which the electric field exceeds 4-MV/m is 1.5m wide. Thus, the vertical extent of the region within which ambient electrons can run away is 1.5 m and it moves with the leader tip downward, illuminating progressively lower sections of the channel. Interestingly, Shaal et al. [48], using a pinhole X-ray camera, estimated the maximum radii of the descending energetic radiation source region associated with leaders in rocket-and-wire triggered lightning to be between 2 and 3 m. This finding seems to be consistent with our estimate of the spatial extent of the strong (>4 MV/m) field region associated with the subsequent-stroke leader represented in Fig. 10. Overall, it appears that an electron accelerator that is pushed along the preconditioned but decayed channel by the downward-extending leader can explain the fact that subsequent-stroke leaders (particularly dart leaders moving without discernible steps) can produce energetic radiation,

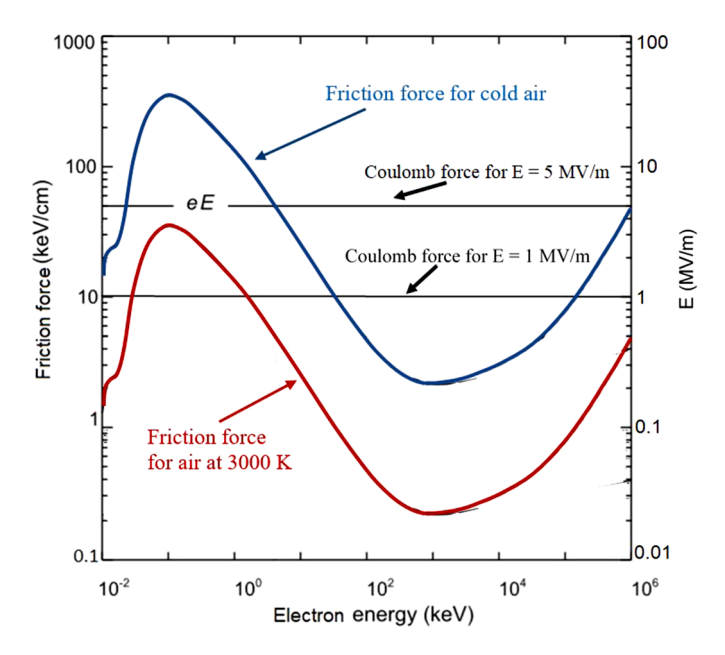


**Fig. 9.** The dynamic friction curves showing the friction force (rate of energy loss per unit distance) experienced by an electron as a function of electron energy for cold air (blue) and for air at 3000 K (red). The curves include the effects of both inelastic scattering of the electron with air molecules and bremsstrahlung emission. The horizontal lines represent the Coulomb force acting on the electron (eE, where E is the electric field intensity and e is the electron charge) corresponding to E=1 MV/m and E=5 MV/m (see the right vertical scale). Electrons can run away when the Coulomb force is greater than the friction force. For cold air (blue curve) and E=5 MV/m, only electrons with energy greater than 5 keV (much higher than the energy of ambient electrons, which does not exceed 30 eV or so) can run away, while for the air at 3000 K (red curve, whose peak corresponds to about 4 MV/m) all free electrons can do so. Adapted from Dwyer [15] and Kereszy et al. [30]. (For interpretation of the references to colour in this figure legend, the reader is referred to the web version of this article.)

although other factors (e.g., super-fields near streamer heads) probably also play a role. Note that leader steps produce both corona streamer bursts and transient E-field changes, and that the latter can briefly enhance the field of the steadily extending leader channel, illustrated in Fig. 10.

We now discuss the likelihood of significant avalanche multiplication of runaway electrons in the scenario in which ambient electrons are accelerated to relativistic speeds in non-luminous but still warm channels (see row 3 in Table 1). This could be done by comparing the extent of the strong (>4 MV/m) E-field region with the distance ( $\lambda$ ) required for an e-fold increase in the number of runaway electrons. Unfortunately, the information on that distance for such high electric fields is presently unavailable. Still, some reasonable estimates can be made. Babich [2] presented the calculated values of  $\lambda$  for different values of "overvoltage" which he defined as  $\delta = E/[217(N/N_0)]$ , where E is the electric field strength in kV/m, N is the density of the gas medium in question,  $N_0$  is the air density under normal conditions, and 217 represents the breakeven electric field (in kV/m), corresponding to the minimum of the friction curve, for air under normal conditions. In our case, the medium in question is air at 3000 K, so that  $N/N_0 = 0.1$  and  $\delta = E/21.7$ .

Values of  $\lambda$  (along with other parameters) as a function of  $\delta$  are given by Babich [2] (see his Table 3) up to  $\delta = 100$ , which corresponds to 22 MV/m for cold air and 2.2 MV/m for air at 3000 K (N/N<sub>0</sub> = 0.1). For  $\delta$  = 100,  $\lambda = 0.16$  m, with the corresponding e-folding time of avalanche enhancement of 0.6 ns, the relativistic runaway electron energy threshold of 1.6 keV, and the average electron energy of 3.46 MeV. There is a clear trend for  $\lambda$  to decrease with increasing  $\delta$ , so for E=4MV/m  $\lambda$  should be smaller than 0.16 m (computed for 2.2 MV/m; N/N<sub>0</sub> = 0.1). Within the estimated 1.5 m extent of the strong (>4 MV/m) E-field region, there will be more than 10 e-folding distances, which means that each runaway electron can produce more than  $2 \times 10^4$  (e<sup>10</sup>) new runaway electrons within that region. Note that the runaway avalanche velocity, about 0.9c [2], where c is the speed of light, is more than a factor of 50 higher than 0.017c (5  $\times$  10<sup>6</sup> m/s), the velocity of the leader tip for the event represented in Fig. 10. As a result, the avalanche will extend beyond the strong (>4 MV/m) E-field region before it eventually decays. For example, for the event represented in Fig. 10, the

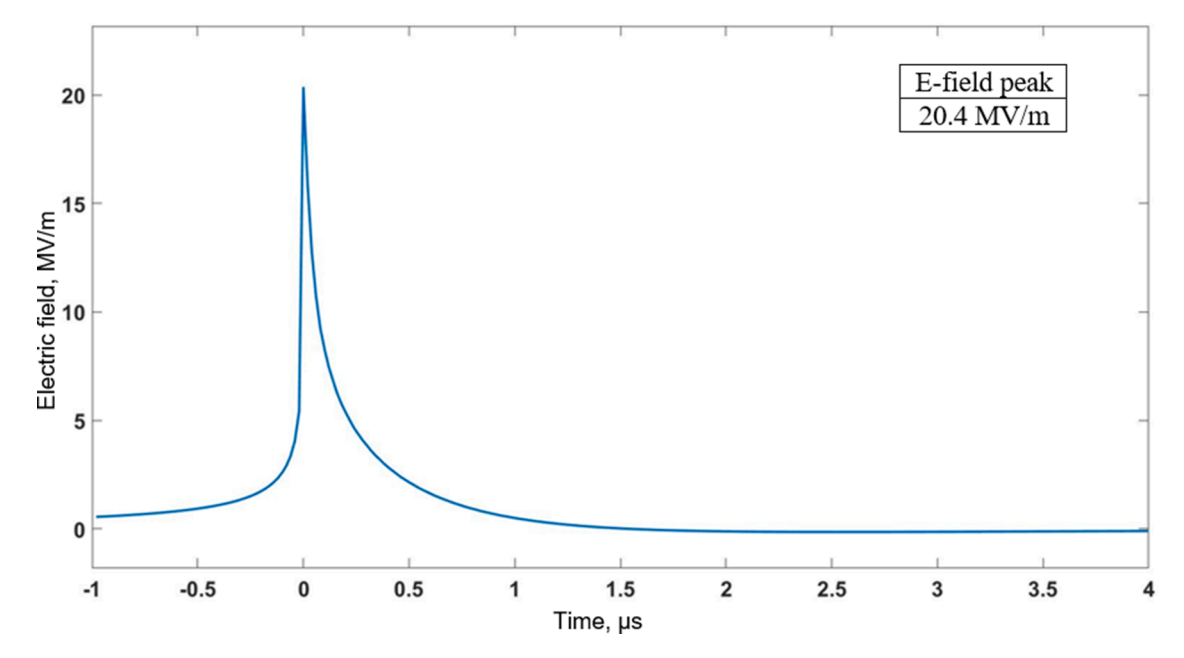


Fig. 10. Calculated electric field waveform at a fixed observation point at an altitude of 150 m above ground level as the descending leader tip passes through that point at t=0. At t<0, the leader tip is above the observation point and at t>0 below it. The following model input parameters were used: prospective return-stroke peak current  $I_p=55$  kA, height of the upper end of the channel above ground level H=7.5 km (electric field is insensitive to this parameter), and leader speed  $v=5\times10^6$  m/s. The leader stepping process was not included in the model. The electric field waveform does not change much if the observation point height is increased to 750 m. Full time scale is 5  $\mu$ s. Adapted from Kereszy et al. [31].

width of the spatial E-field pulse at the 2 MV/m level is 3.6 m. Thus, runaway electron multiplication should be expected not only inside the 1.5-m region, but also ahead of that region, as long as the decreasing E-field remains above the level (a few hundred kV/m) sufficient for accelerating runaway electrons in a warm (reduced air-density) channel, thereby enlarging the size of the energetic radiation source.

It is important to note that the above discussion of acceleration and multiplication of runaway electrons is with reference to the unusually intense (peak current = 55 kA) subsequent stroke represented in Fig. 3 (lower panel) and Fig. 10. For typical subsequent strokes (peak currents in the 10 to 15 kA range), the peak of the E-field waveform associated with the descending leader tip is between 2 and 3 MV/m [31], which is lower than needed to overcome the friction curve peak (see Fig. 9, red curve). The observed dependence of the occurrence/detectability of energetic radiation on the RS peak current is as follows. Mallick et al. [36] reported that only 50% of natural-lightning events (both first and subsequent strokes combined) with peak currents in the 10-40 kA range produced detectable X-rays vs. 100% for the 40–60 kA range. Similarly, Tran et al. [52] reported 23%, 83%, and 100% for the 4-40 kA, 40-60 kA, and 60-140 kA ranges, respectively. Saba et al. [46] observed four natural-lightning strokes in the same channel some hundreds of meters from the detector, only one of which produced detectable X-rays; its estimated peak current was 38 kA vs. 6 to 12 kA for the other three strokes. The X-ray producer was the second stroke in the channel and was initiated by dart leader. For the four strokes in Saba et al.'s study, the detection efficiency was 25%. For rocket-and-wire triggered lightning (containing only subsequent-type strokes), the occurrence/detectability of X-rays appears to be higher than for natural lightning (about 80% for all peak currents, up to 40 kA or so, combined), possibly due to detectors being usually within a few tens of meters of the source vs. hundreds of meters or more for natural lightning. Note that some electrons can "tunnel" through the friction-curve barrier when the field is well below the so-called cold runaway threshold, as discussed in [14].

The observational fact that not all leader steps are associated with X-ray bursts (see, for example, Fig. 4) can be explained, among other things, by channel tortuosity, such that some steps produce insufficient X-ray flux in the direction of the detector. For the case of dart leader, Saba et al. [46] presented evidence that channel sections directed toward the detector are more likely to produce detectable X-rays.

Further studies, including detailed modeling of X-ray/gamma-ray production, are needed to see if the elevated-temperature scenario (see next to the last row of Table 1) can quantitatively explain the ground-based observations of energetic radiation (including its energy spectrum) from subsequent leaders traversing pre-conditioned channels to ground, as well as downward TGFs occurring in the presence of decayed channels/branches in the cloud.

We now discuss the context in which downward TGFs occur. TGFs observed to date at ground level in Florida (a total of five) all occurred well after the flash initiation processes. In contrast, Belz et al. [4], from recent ground-based observations at 1.4 km above sea level in Utah, reported TGFs associated with the preliminary breakdown (PB) process, when there was undisturbed (cold) air between the cloud base and ground. TGFs recorded in a similar context at ground level during winter thunderstorms in Japan were reported by Wada et al. [56], and Hisadomi et al. [26]. The lack of observations of TGFs associated with the preliminary breakdown process in Florida could be related to the larger altitude of lightning initiation above the sea-level terrain in Florida compared to the 1.4-km elevated terrain in Utah and to low-altitude winter thunderclouds in Japan. It is not clear why no TGFs occurring well after the cloud-to-ground lightning initiation process; that is, when there exists a strong (hot-channel; [17,18,25,53]) or weak (decayed-channel; [30]) electric connection to ground, were reported from the studies in Utah and Japan. All TGFs observed in Florida occurred in the presence of lightning channels/branches at different stages of development or decay, which suggests that the elevated-temperature scenario of X-ray/gamma-ray production discussed above could be involved.

#### 5. Summary and concluding remarks

- 1 All types of negative lightning leaders, whether they exhibit discernible stepping or not, can produce energetic radiation. Some subsequent-stroke leaders are more prolific X-ray/gammaray producers than their corresponding first-stroke leaders.
- 2 The energy of individual photons associated with the stepping of either first (stepped) or subsequent (dart-stepped) leaders can exceed several MeV.
- 3 Besides leader stepping, energetic radiation has been observed during collisions of opposite-polarity streamers at the onset of the breakthrough phase of the lightning attachment process.
- 4 TGFs can be observed either from space (upward TGFs) or from ground (downward TGFs). To date, downward TGFs were observed in Florida, Utah, and Japan.
- 5 Downward TGFs observed in Florida (a total of five to date) occurred either in the presence of steady current carrying negative charge to ground or during the initial stage of a subsequent-stroke leader; that is, in all the cases well after the flash-initiation process.
- 6 In contrast, Belz et al. [4], from recent ground-based observations in Utah (1.4 km above sea level), reported TGFs associated with the preliminary breakdown; that is, during the flash-initiation process. Similar observations were reported for winter lightning in Japan.
- 7 The reasons for the disparity between TGF observations in Florida on the one hand and in Utah and Japan on the other hand are presently not clear. Further research is needed to better understand the lightning processes giving rise to TGFs recorded at ground level.
- 8 There are three factors/scenarios that can lead to acceleration and multiplication of runaway electrons: (1) super-high electric field (much higher than the conventional breakdown value), (2) energetic electrons supplied by external sources (cosmic rays), and (3) elevated air temperature (reduced air density).
- 9 Subsequent-stroke leaders traverse elevated-temperature (3000 K or so) channels and are capable of producing short electric field pulses with peaks up to several MV/m and more. Such fields are sufficient for acceleration of ambient electrons over the friction-curve maximum to the keV range and further to relativistic energies needed for production of X-ray/gamma-ray emissions. Significant avalanching of runaway electrons seems to be possible.
- 10 Further studies, including detailed modeling of X-ray/gamma-ray production, are needed to see if the elevated-temperature scenario can quantitatively explain the ground-based observations of energetic radiation (including its energy spectrum) from subsequent leaders traversing pre-conditioned channels to ground, as well as downward TGFs occurring in the presence of decayed channels/branches in the cloud.

#### Data availability

This is a review paper. All the presented data are found in published papers referred to herein.

#### **Declaration of Competing Interest**

The authors declare that they have no known competing financial interests or personal relationships that could have appeared to influence the work reported in this paper.

#### **Data Availability**

No data was used for the research described in the article.

#### Acknowledgements

This work was supported in part by the U.S. National Science Foundation grant AGS-2114471. The authors thank J.R. Dwyer for providing the NaI X-ray/gamma-ray detector operating at LOG and for useful discussions. Over the years, many researchers contributed significantly to LOG operations; their names appear in the text and in the list of references of this paper.

#### References

- Y. Baba, V.A. Rakov, Electromagnetic fields at the top of a tall building associated with nearby lightning return strokes, IEEE Trans. Electromagn. Compat. 49 (3) (2007) 632–643, https://doi.org/10.1029/2006JD007222.
- [2] L.P. Babich, Relativistic runaway electron avalanche, Physics Uspekhi, 63 (12) (2020) 1188–1218, https://doi.org/10.3367/UFNe.2020.04.038747.
- [3] K.I. Bakhov, L.P. Babich, I.M. Kutsyk, Temporal characteristics of runaway electrons in electron-neutral collision-dominated plasma of dense gases: monte Carlo calculations, IEEE Trans. Plasma Sci. 28 (4) (2000) 1254–1262.
- [4] J.W. Belz, P.R. Krehbiel, J. Remington, M.A. Stanley, R.U. Abbasi, R. LeVon, et al., Observations of the origin of downward terrestrial gamma-ray flashes, J. Geophys. Res. Atmosph. 125 (23) (2020), https://doi.org/10.1029/2019JD031940.
- [5] Bowers, et al., Combining Cherenkov and scintillation detector observations with simulations to deduce the nature of high-energy radiation excesses during thunderstorms, Phys. Rev. D 100 (2019), 043021, https://doi.org/10.1103/ PhysRevD.100.043021.
- [6] M.S. Briggs, G.J. Fishman, V. Connaughton, P.N. Bhat, W.S. Paciesas, R.D. Preece, et al., First results on terrestrial gamma ray flashes from the fermi gamma-ray burst monitor, J. Geophys. Res. 115 (A7) (2010) A07323, https://doi.org/10.1029/2001A015242
- [7] J.L. Burnett, I.W. Croudace, P.E. Warwick, Short-lived variations in the background gamma-radiation dose, J. Radiol. Prot. 30 (2010) 525–533, https://doi.org/ 10.1088/0952-4746/30/3/007.
- [8] A. Chilingarian, A. Daryan, K. Arakelyan, A. Hovhannisyan, B. Mailyan, L. Melkumyan, G. Hovsepyan, S. Chilingaryan, A. Reymers, L. Vanyan, Groundbased observations of thunderstorm-correlated fluxes of high-energy electrons, gamma rays, and neutrons, Phys. Rev. D 82 (2010), 043009.
- [9] A. Chilingarian, G. Hovsepyan, L. Kozliner, Thunderstorm ground enhancements: gamma ray differential energy spectra, Phys. Rev. D 88 (2013), 073001.
- [10] A. Chilingarian, Y. Khanikyants, E. Mareev, D. Pokhsraryan, V.A. Rakov, S. Soghomonyan, Types of lightning discharges that abruptly terminate enhanced fluxes of energetic radiation and particles observed at ground level, J. Geophys. Res. Atmos. 122 (2017) 7582–7599, https://doi.org/10.1002/2017JD026744.
- [11] A. Chilingarian, Y. Khanikyants, V.A. Rakov, S. Soghomonyan, Termination of thunderstorm-related bursts of energetic radiation and particles by inverted intracloud and hybrid lightning discharges, Atmos. Res. 223 (2020), 104713, https://doi.org/10.1016/j.atmosres.2019.104713.
- [12] V. Cooray, M. Becerra, V.A. Rakov, On the electric field at the tip of dart leaders in lightning flashes, J. Atmos. Sol. Terr. Phys. 71 (12) (2009) 1397–1404, https://doi. org/10.1016/j.jastp.2009.06.002.
- [13] V. Cooray, J.R. Dwyer, V.A. Rakov, M. Rahman, On the mechanism of X-ray production by dart leaders of lightning flashes, J. Atmos. Sol. Terr. Phys. 72 (11–12) (2010) 848–855, https://doi.org/10.1016/j.jastp.2010.04.006.
- [14] G.S. Diniz, C. Rutjes, U. Ebert, I.S. Ferreira, Cold electron runaway below the friction curve, J. Geophys. Res. Atmosph. 124 (2019) 189–198, https://doi.org/ 10.1029/2018/ID029178.
- [15] J.R. Dwyer, Implications of x-ray emission from lightning, Geophys. Res. Lett. 31 (2004) L12102, https://doi.org/10.1029/2004GL019795.
- [16] J.R. Dwyer, H.K. Rassoul, M. Al-Dayeh, L. Caraway, B. Wright, A. Chrest, et al., Measurements of X-ray emission from rocket-triggered lightning, Geophys. Res. Lett. 31 (5) (2004) L05118. https://doi.org/10.1029/2003GL018770.
- [17] J.R. Dwyer, H.K. Rassoul, M. Al-Dayeh, L. Caraway, B. Wright, A. Chrest, et al., A ground level gamma-ray burst observed in association with rocket-triggered lightning, Geophys. Res. Lett. 31 (5) (2004) L05119, https://doi.org/10.1029/ 2003GL018771.
- [18] J.R. Dwyer, M.M. Schaal, E. Cramer, S. Arabshahi, N. Liu, H.K. Rassoul, et al., Observation of a gamma-ray flash at ground level in association with a cloud-toground lightning return stroke, J. Geophys. Res. 117 (A10) (2012) A10303, https://doi.org/10.1029/2012JA017810.
- [19] J.R. Dwyer, et al., X-ray bursts associated with leader steps in cloud-to-ground lightning, Geophys. Res. Lett. 32 (2005) L01803, https://doi.org/10.1029/ 2004GL021782.
- [20] J.R. Dwyer, M. Schaal, H.K. Rassoul, M.A. Uman, D.M. Jordan, D. Hill, High-speed X-ray images of triggered lightning dart leaders, J. Geophys. Res. 116 (2011) D20208, https://doi.org/10.1029/2011JD015973.
- [21] J.R. Dwyer, M.A. Uman, The physics of lightning, Phys. Rep. 534 (2014) 147–241.
- [22] K.B. Eack, W.H. Beasley, Long-duration X-ray emissions observed in thunderstorms, J. Geophys. Res. Atmos. 120 (2015) 6887–6897, https://doi.org/ 10.1002/2015JD023262.
- [23] G.J. Fishman, P.N. Bhat, R. Mallozzi, J.M. Horack, T. Koshut, C. Kouveliotou, et al., Discovery of intense gamma-ray flashes of atmospheric origin, Science 264 (5163) (1994) 1313–1316, https://doi.org/10.1126/science.264.5163.1313.

- [24] A.V. Gurevich, G.M. Milikh, R. Roussel-Dupre, Runaway electron mechanism of air breakdown and preconditioning during a thunderstorm, Phys. Lett. A 165 (1992) 462, 468
- [25] B.M. Hare, M.A. Uman, J.R. Dwyer, D.M. Jordan, M.I. Biggerstaff, J.A. Caicedo, et al., Ground-level observation of a terrestrial gamma-ray flash initiated by a triggered lightning, J. Geophys. Res. Atmosph. 121 (11) (2016) 6511–6533, https://doi.org/10.1002/2015JD024426.
- [26] S. Hisadomi, K. Nakazawa, Y. Wada, Y. Tsuji, T. Enoto, T. Shinoda, et al., Multiple gamma-ray glows and a downward TGF observed from nearby thunderclouds, J. Geophys. Res. Atmosph. 126 (18) (2021), https://doi.org/10.1029/ 2021JD034543 e2021JD034543.
- [27] J. Howard, M.A. Uman, J.R. Dwyer, D. Hill, C. Biagi, Z. Saleh, et al., Co-location of lightning leader X-ray and electric field change sources, Geophys. Res. Lett. 35 (2008) L13817, https://doi.org/10.1029/2008GL034134.
- [28] J. Howard, M.A. Uman, C. Biagi, D. Hill, J. Jerauld, V.A. Rakov, et al., RF and X-ray source locations during the lightning attachment process, J. Geophys. Res. 115 (2010) D06204, 10.1029/2009JD012055.
- [29] N.A. Kelley, et al., Relativistic electron avalanches as a thunderstorm discharge competing with lightning, Nat. Commun 6 (2015) 7845.
- [30] I. Kereszy, V.A. Rakov, Z. Ding, J.R. Dwyer, Ground-based observation of a TGF occurring between opposite polarity strokes of a bipolar cloud-to-ground lightning flash, J. Geophys. Res. Atmosph. 127 (2022), https://doi.org/10.1029/2021JD036130 e2021JD036130.
- [31] I. Kereszy, V.A. Rakov, L. Czumbil, A. Muresan, Z. Ding, D. Micu, V. Cooray, Energetic radiation from subsequent-stroke leaders: the role of reduced air density in decayed lightning channels, Appl. Sci., Special Issue "Physics Principles, Measure. Characteristics Lightning 12 (2022) 7520, https://doi.org/10.3390/ app12157520.
- [32] P. Kochkin, A.P.J. van Deursen, M. Marisaldi, A. Ursi, A.I. de Boer, M. Bardet, N. Østgaard, In-flight observation of gamma ray glows by ILDAS, J. Geophys. Res. Atmosph. 122 (2017) 12801–12811, https://doi.org/10.1002/2017JD027405.
- [33] A.Y. Kostinskiy, V.S. Syssoev, N.A. Bogatov, E.A. Mareev, M.G. Andreev, M. U. Bulatov, et al., Abrupt elongation (stepping) of negative and positive leaders culminating in an intense corona streamer burst: observations in long sparks and implications for lightning, J. Geophys. Res. Atmosph. 123 (2018) 5360–5375, https://doi.org/10.1029/2017JD027997.
- [34] F. Lyu, S.A. Cummer, L. McTague, Insights into high peak current in-cloud lightning events during thunderstorms, Geophys. Res. Lett. 42 (16) (2015) 6836–6843. https://doi.org/10.1002/201501065047.
- [35] B.G. Mailyan, M.S. Briggs, E.S. Cramer, G. Fitzpatrick, O.J. Roberts, M. Stanbro, V. Connaughton, S. McBreen, P.N. Bhat, J.R. Dwyer, The spectroscopy of individual terrestrial gamma-ray flashes: constraining the source properties, J. Geophys. Res. Space Physics 121 (2016) 11346–11363, https://doi.org/10.1002/2016JA022702.
- [36] S. Mallick, V.A. Rakov, J.R. Dwyer, A study of X-ray emissions from thunderstorms with emphasis on subsequent strokes in natural lightning, J. Geophys. Res. 117 (2012) D16107, https://doi.org/10.1029/2012JD017555.
- [37] M. McCarthy, G.K. Parks, Further observations of X-rays inside thunderstorms, Geophys. Res. Lett. 12 (1985) 393–396, https://doi.org/10.1029/ GL012i006p00393.
- [38] C.B. Moore, K.B. Eack, G.D. Aulich, Energetic radiation associated with lightning stepped leaders, Geophys. Res. Lett. 28 (11) (2001) 2141–2144, https://doi.org/ 10.1029/2001GI.013140.
- [39] G. Moss, V.P. Pasko, N. Liu, G. Veronis, Monte Carlo model for analysis of thermal runaway electrons in streamer tips in transient luminous events and streamer zones of lightning leaders, J. Geophys. Res. 111 (2006) A02307, https://doi.org/ 10.1029/2005JA011350.
- [40] T. Neubert, N. Ostgaard, V. Reglero, O. Chanrion, M. Heumesser, K. Dimitriadou, et al., Terrestrial gamma-ray flashes and ionospheric UV emissions generated by lightning, Science 367 (6474) (2020) 183–186, https://doi.org/10.1126/science.aax3872
- [41] J. Paatero, J. Hatakka, Wet deposition efficiency of short-lived radon-222 progeny in central Finland, Boreal Environ. Res. 4 (1999) 285–293.
- [42] V.A. Rakov, Lightning flashes transporting both negative and positive charges to ground, in: C. Pontikis (Ed.), Recent Progresses in Lightning Physics, Research Signpost, 2005, pp. 9–21.
- [43] V.A. Rakov, I. Kereszy, Ground-based Observations of Lightning-Related X-Ray and Gamma-Ray Emissions in Florida, Colombo, Sri Lanka, 2021, p. 2 (Invited Lecture), ICLP-SIPDA 2021.
- [44] Rakov, V.A. and M.D. Tran (2019). The breakthrough phase of lightning attachment process: from collision of opposite-polarity streamers to hot-channel connection, Electr. Power Syst. Res., 173, 122–134, https://doi.org/10.1016/j. epsr.2019.03.018.
- [45] V.A. Rakov, M.A. Uman, Lightning: Physics and Effects, Cambridge University Press, 2003.
- [46] M.M.F. Saba, M.A.S. Ferro, E.T. Cuadros, D.M. Custódio, A. Nag, C. Schumann, et al., High-speed video observation of a dart leader producing X-rays, J. Geophys. Res. Space Phys. 124 (2019) 10564–10570, https://doi.org/10.1029/2019JA027247.
- [47] Z. Saleh, J. Dwyer, J. Howard, M. Uman, M. Bakhtiari, D. Concha, M. Stapleton, D. Hill, C. Biagi, H. Rassoul, Properties of the X-ray emission from rocket-triggered lightning as measured by the Thunderstorm Energetic Radiation Array (TERA), J. Geophys. Res. 114 (2009) D17210, https://doi.org/10.1029/2008JD011618.
- [48] M.M. Schaal, et al., The structure of X-ray emissions from triggered lightning leaders measured by a pinhole-type X-ray camera, J. Geophys. Res. Atmos. 119 (2014) 982–1002, https://doi.org/10.1002/2013JD020266.

- [49] D.M. Smith, L.I. Lopez, R.P. Lin, C.P. Barrington-Leigh, Terrestrial gamma-ray flashes observed up to 20 MeV, Science 307 (5712) (2005) 1085–1088, https://doi. org/10.1126/science.1107466.
- [50] D.M. Suszcynsky, R. Roussel-Dupre, G. Shaw, Ground-based search for X rays generated by thunderstorms and lightning, J. Geophys. Res. 101 (D18) (1996) 23505–23516, https://doi.org/10.1029/96JD02134.
- [51] T. Torii, et al., Migrating source of energetic radiation generated by thunderstorm activity, Geophys. Res. Lett. 38 (2011) L24801, https://doi.org/10.1029/ 2011GL049731.
- [52] M.D. Tran, I. Kereszy, V.A. Rakov, J.R. Dwyer, On the role of reduced air density along the lightning leader path to ground in increasing X-ray production relative to normal atmospheric conditions, Geophys. Res. Lett. 46 (2019) 9252–9260, https:// doi.org/10.1029/2019GL083753.
- [53] M.D. Tran, V.A. Rakov, S. Mallick, J.R. Dwyer, A. Nag, S. Heckman, A terrestrial gamma-ray flash recorded at the Lightning Observatory in Gainesville, Florida, J. Atmosph. Solar-Terrestrial Phys. 136 (A) (2015) 86–93, https://doi.org/ 10.1016/j.jastp.2015.10.010.

- [54] H. Tsuchiya, et al., Detection of high-energy gamma rays from winter thunderclouds, Phys. Rev. Lett. 111 (2013), 015001.
- [55] M.A. Uman, R.E. Voshall, Time interval between lightning strokes and the initiation of dart leaders, J. Geophys. Res. 73 (2) (1968) 497–506, https://doi.org/ 10.1029/JB073i002p00497.
- [56] Y. Wada, T. Enoto, Y. Nakamura, et al., Gamma-ray glow preceding downward terrestrial gamma-ray flash, Commun. Phys. 2 (2019) 67, https://doi.org/10.1038/ s42005-019-0168-y.
- [57] Y. Wada, T. Enoto, Y. Nakamura, T. Morimoto, M. Sato, T. Ushio, et al., High peak-current lightning discharges associated with downward terrestrial gamma-ray flashes, J. Geophys. Res. Atmosph. 125 (2020), https://doi.org/10.1029/2019JD031730 e2019JD031730.
- [58] Y. Zhu, V.A. Rakov, M.D. Tran, A study of preliminary breakdown and return stroke processes in high-intensity negative lightning discharges, Atmosphere, Special Issue, Electromagnetic Fields and Waves with Special Attention to Lightning Flashes 7 (2016) 130, https://doi.org/10.3390/atmos7100130, 2016.